Journal of Glaciology

Article

Cite this article: Shan Q, Fan K, Liu J (2024). The stepwise decrease of 4+ year ice extent and its linked survivability since around 2007. *Journal of Glaciology* **70**, e85, 1–11. https://doi.org/10.1017/jog.2024.33

Received: 2 October 2023
Revised: 28 March 2024
Accepted: 4 April 2024

Keywords:
climate change; ice and climate; sea ice

Corresponding author:
Ke Fan; Email: fank8@mail.sysu.edu.cn

cambridge.org/jog

The stepwise decrease of 4+ year ice extent and its linked survivability since around 2007

Qi Shan[1,3], Ke Fan[2] and Jiping Liu[2]

[1]Institute of Atmospheric Physics, Chinese Academy of Sciences, Beijing 100029, China; [2]School of Atmospheric Sciences, Sun Yat-sen University, and Southern Marine Science and Engineering Guangdong Laboratory (Zhuhai), Zhuhai 519082, China and [3]University of the Chinese Academy of Sciences, Beijing 100049, China

Abstract

Recent studies have reported a shift in the Arctic sea ice to a younger state after around 2007. This study reveals that this shift can be primarily attributed to a stepwise-type reduction in the extent of 4 years or older (4+ year) ice and its linked survivability. After this shift, the fraction of 4+ year ice extent relative to the total ice changed from 30.5 to 10.0%. Sea-ice survivability can serve as a key indicator of sea-ice persistence in response to other factors. We demonstrate that the decrease of 4+ year ice is controlled by the decrease of its linked survivability in a non-linear manner, signifying small alterations in the survivability can result in relatively large changes in the extent of 4+ year ice. The decrease in survivability is affected by both winter and summer processes. Summer melting contributed the most, while the contribution of the export through Fram Strait was minor. However, the significant rise in residual loss during the growth season suggests that other winter processes may also have played an important role.

1. Introduction

Sea ice is critical in the energy budget and the exchange of heat and momentum between the atmosphere and ocean, and thus the ecosystem in the Arctic (Thomas, 2017). Based on whether it has survived at least one summer melt season, sea ice can be classified into two categories: first-year ice (FYI) and multi-year ice (MYI). Due to longer growth periods and more deformation processes, MYI is thicker, stronger, less salty and rougher than FYI (Bi and others, 2020). These contrasting characteristics may lead to divergent feedback mechanisms and climate implications.

During the past few decades, the Arctic sea-ice coverage has shrunk rapidly, with a faster rate of loss for the MYI than for the total ice (Maslanik and others, 2011; Comiso, 2012; Liu and others, 2019). Investigating the changes and underlying drivers of MYI coverage is of great importance. On the one hand, sea-ice age (SIA) can be used as a proxy for thickness (Maslanik and others, 2007; Tschudi and others, 2016). This correspondence can also be supported by the strong correlation between the MYI area and the total ice volume in the satellite product (Kwok, 2018). On the other hand, the decrease in MYI could provide more area for sea water to freeze into FYI during winter (Zhao and others, 2023).

The changes in MYI coverage can be considered as controlled by its survivability, which describes the likelihood of sea ice persisting throughout a growth–melt cycle (Armour and others, 2011; Tooth and Tschudi, 2018). The survivability serves as an indicator of sea-ice response to climate forcing. For the MYI coverage, the survivability can be affected by both thermodynamic and dynamic processes, including summer melting, export through Fram Strait (FS) and ridging (e.g. Kwok, 2007, 2015; Kwok and Cunningham, 2010; Babb and others, 2023, hereafter B23; Regan and others, 2023), but separating their respective contributions is challenging.

In addition to gradually shrinking in response to global warming, emerging studies indicate the Arctic sea ice can show stepwise-type regime shifts. Sumata and others (2023) revealed an abrupt stepwise shift around 2007 from an 'old, thick, deformed ice regime' to a 'younger, thinner, more uniform ice regime' in the Arctic by continuous monitoring data in FS since 1990. Moore and others (2022) reported a similar shift in the western Arctic sea ice. Additionally, B23 found that the MYI area experienced two stepwise reductions in 1989 and around 2007, respectively. They indicated that the former reduction was primarily driven by export, while the latter was attributed to a combination of export, melt and replenishment. Moreover, this regime shift around 2007 is also manifested in other aspects of Arctic climate, including an intensified response of the volume flux through FS to variation in Arctic sea-ice volume after 2007 (Yang and others, 2023) and a transition in Arctic Dipole mode from a near-neutral phase to a positive phase around 2007 (Polyakov and others, 2023).

In this study, we will first show another stepwise variation around 2007, that is, the decrease of the extent of sea ice aged 4 years or older (4+ year ice) in the Arctic Basin, and demonstrate how it is controlled by the decrease of survivability. Subsequently, we will estimate the individual contribution of various processes to the decrease of survivability. The paper is structured as follows. Section 2 presents the data employed and the definition of sea-ice survivability. Section 3 introduces how we budget sea-ice survivability. Section 4 outlines the results of our analysis. Section 5 presents a discussion of our results. The final section provides a summary.

2. Data and method

2.1 Data

Here we use version 4 of the SIA dataset from the National Snow and Ice Data Center (NSIDC; Tschudi and others, 2019a). The NSIDC-SIA dataset is derived by tracking ice parcels in a Lagrangian sense using sea-ice motion (SIM) data and recording their age. In particular, each gridcell that contains ice in NSIDC-SIA data was advected and tracked as a Lagrangian parcel at weekly time steps. If the sea-ice concentration (SIC) at each gridcell is ≥15% throughout the entire melt season, the gridcell is considered to have survived the summer melting, and its age increases by one. Therefore, SIA will add one at the end of summer, and it is a discrete value. Furthermore, if several ice parcels propagated into the same gridcell, the age of the oldest parcel is assigned to that gridcell. The version 4 NSIDC-SIA dataset has eliminated errors created by artificial ice divergence in the previous version (Tschudi and others, 2020). Furthermore, Ye and others (2023) have demonstrated its ability to generally discriminate between MYI and FYI. The dataset we used is in a 12.5 km × 12.5 km Equal-Area Scalable Earth (EASE) grid and available weekly from 1984 to 2022. The distribution of SIA during the period 1985–2022 is illustrated in Figure 1 and our analysis will be limited to the Arctic Basin defined in the bottom right corner of Figure 1, as MYI predominantly exists in this region.

We also use the NSIDC SIM (Tschudi and others, 2019b) and SIC (DiGirolamo and others, 2022) datasets. The SIM and the SIC data are originally in a 25 km × 25 km EASE grid and NSIDC polar stereographic grid, respectively. Both datasets were then interpolated using the bilinear method to 12.5 km × 12.5 km EASE grid, facilitating subsequent calculations with SIA. The SIM data are weekly as the SIA data, while the SIC data are every other day from 26 October 1978 to 9 July 1987 and daily afterwards. Additionally, monthly 2 m temperature and sea-level pressure in the fifth-generation global reanalysis produced by ECMWF (ERA5; Hersbach and others, 2020) were used in this study.

2.2 Sea-ice survivability

The week that SIA increases (hereafter called the start week) varies each year (Fig. S1), with an average occurring around the 37th week. We defined one growth–melt cycle as from the start week to the week preceding the start week in the following year. The increase in SIA for a specific ice parcel signifies its survival over the last growth–melt cycle. Following Armour and others (2011), we can estimate sea-ice survivability by the survival ratio of sea-ice extent (SIE), which is expressed as follows:

$$\beta_{i,n} = SIE_{i+1,\,(n,\,St^{\mathrm{th}})}/SIE_{i,\,(n-1,\,St^{\mathrm{th}})} \tag{1}$$

where i is the age of ice, n is the year, $\beta_{i,\,n}$ represents the survival ratio of ice aged i in year n and $SIE_{i+1,\,(n,\,St^{\mathrm{th}})}$ represents the extent of sea ice aged $i+1$ in the start week of year n. For example, if all the 2 year ice in the start week of 1999 can persist until the start week of 2000 and become 3 year ice. The ratio between $SIE_{3,\,(2000,\,St^{\mathrm{th}})}$ and $SIE_{2,\,(1999,\,St^{\mathrm{th}})}$ is 1, i.e. the survival ratio of 2 year ice in 2000 ($\beta_{2,\,2000}$).

The survival ratio in one complete growth–melt cycle, $\beta_{i,\,n}$, can be further divided into the survival ratio in the growth season, $\beta_{i,\,n}^{\mathrm{growth}}$, and the survival ratio in the melt season, $\beta_{i,\,n}^{\mathrm{melt}}$. It is found the total SIE in the Arctic Basin begins to decrease around the 18th week (Fig. S2), indicating the onset of the melt season. Considering that MYI typically melts later than FYI, we have chosen a slightly later period, the 20th–25th weeks, as the boundary between the growth and melt seasons to reduce the sample error (the results are not sensitive to the windows selected here). Then the survival ratio in the growth and melt seasons can be calculated as follows:

$$\beta_{i,\,n}^{\mathrm{growth}} = SIE_{i,\,(n,\,\overline{20^{\mathrm{th}}-25^{\mathrm{th}}})}/SIE_{i,\,(n-1,\,St^{\mathrm{th}})} \tag{2}$$

$$\beta_{i,\,n}^{\mathrm{melt}} = SIE_{i+1,\,(n,\,St^{\mathrm{th}})}/SIE_{i,\,(n,\,\overline{20^{\mathrm{th}}-25^{\mathrm{th}}})} \tag{3}$$

where $SIE_{i,\,(n,\,\overline{20^{\mathrm{th}}-25^{\mathrm{th}}})}$ represents the extent of sea ice aged i averaged over the 20th–25th weeks of year n. Therefore, we will have $\beta_{i,\,n} = \beta_{i,\,n}^{\mathrm{growth}} \times \beta_{i,\,n}^{\mathrm{melt}}$.

3. Budget of sea-ice survivability

As mentioned in Section 1, sea-ice survivability can be influenced by various processes. Here, we mainly focused on the contributions of two processes, summer melting and export through FS, to the loss of MYI extent, while the remaining loss was considered as residual. Furthermore, the budget of total loss during one growth–melt cycle was divided into two parts, growth season and melt season, respectively, as indicated by the following equation:

$$\begin{aligned} Loss_{i,\,n} = & \underbrace{Export^{\mathrm{growth}} + Residual^{\mathrm{growth}}}_{Loss^{\mathrm{growth}}} \\ & + \underbrace{Export^{\mathrm{melt}} + Melting + Residual^{\mathrm{melt}}}_{Loss^{\mathrm{melt}}} \end{aligned} \tag{4}$$

where $Loss_{i,\,n}$ is the loss of i year ice extent in n year, the superscripts growth and melt represent the corresponding loss in the growth and melt seasons, respectively. Greater $Loss_{i,\,n}$ corresponds to lower $\beta_{i,\,n}$, as demonstrated by $\beta_{i,\,n} = 1 - Loss_{i,\,n}/SIE_{i,\,(n-1,\,St^{\mathrm{th}})}$. Similar to Section 2.2, we use the 20th–25th weeks as the boundary between the growth and melt seasons when calculating the loss of MYI extent. For example, the melt analyzed in this paper is the average of melt calculated by treating each week within the 20th–25th weeks as an individual boundary.

3.1 Sea-ice export through FS

We select a zonal gate at 80° N (17° W–16° E, red line in the bottom right corner of Fig. 1) to calculate the sea-ice area fluxes through FS (note that we do not consider the concentration in the calculation). In the calculation, we divide the gate into small segments with a resolution of 1° (~20 km). To reduce the sample error in determining the SIA of each segment, we select the nearest four SIA gridcells of each segment and calculate the area fluxes through each segment using the following equation:

$$F_i = \sum_{j=1}^{4} V_{i,\,j} L/4 \tag{5}$$

where F_i is the area export fluxes of i year ice, j represents the number of four nearest grids for each segment, V represents velocity perpendicular to the segment (here is the meridional velocity) calculated from the NSIDC SIM dataset (Tschudi and others, 2019b) and L is the length of each segment. The total area fluxes through FS are obtained by summing up the fluxes of each segment. The results are not sensitive to the resolution of segments and the number of nearest gridcells (not shown).

3.2 Summer melting

Since quantifying the melt is a challenging task, here we use an indirect method to estimate it. As we can see, sea ice within the

https://doi.org/10.1017/jog.2024.33 Published online by Cambridge University Press

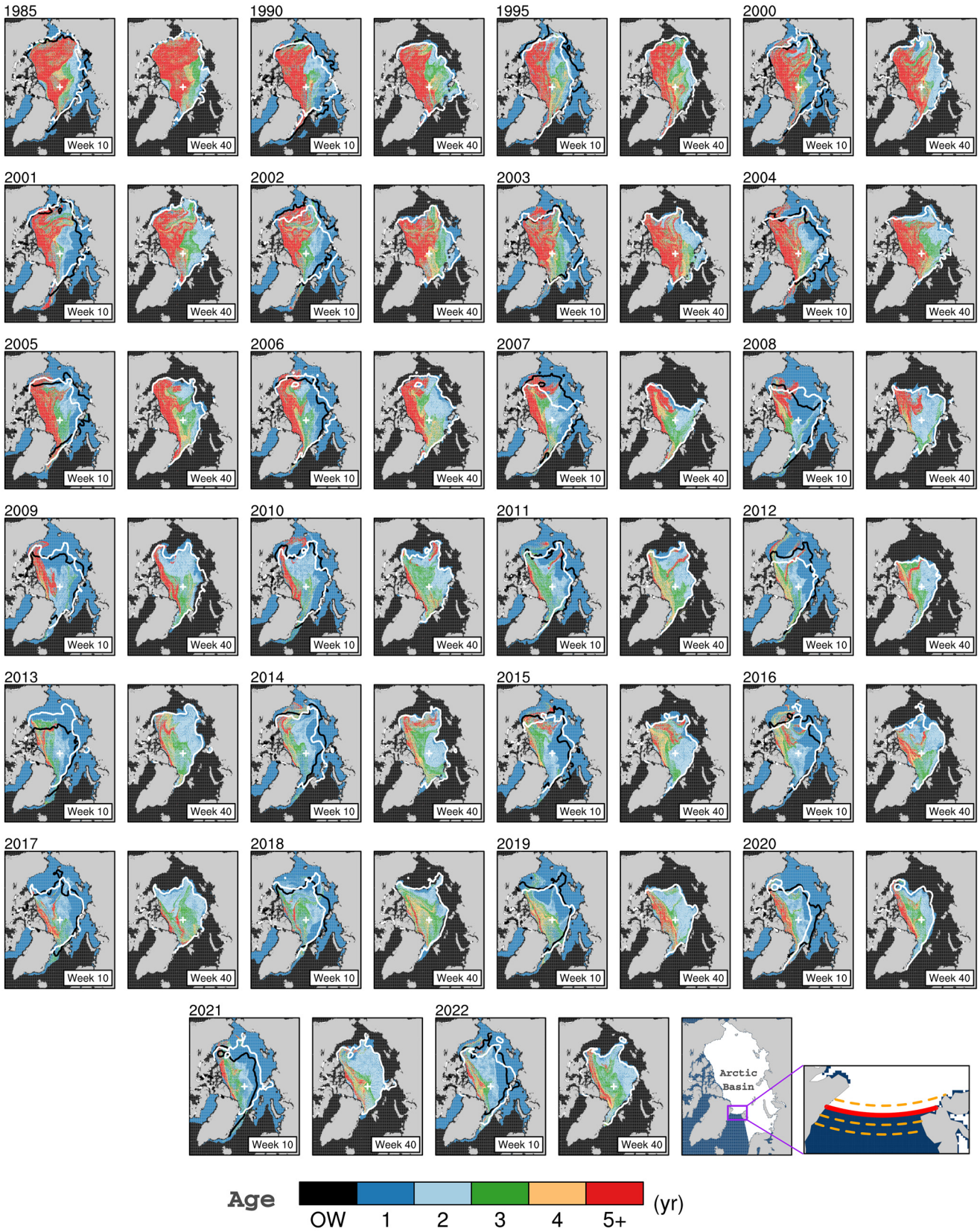

Figure 1. Spatial distribution of Arctic sea ice age (SIA) in 10th and 40th weeks during 1985–2022. The distributions before 2000 are presented every 5 years. The white contours in the 10th and 40th weeks of each year represent the September sea-ice edge in the corresponding year, while the black contours in the 10th week represent the September sea-ice edge in the previous year. The last two figures in the bottom right corner illustrate the Arctic Basin (white shading) used to analyze in our main text, and the gates used to calculate sea-ice area fluxes through Fram Strait, respectively. The solid red line indicates the zonal gate at 80° N, while the orange-dashed lines represent the zonal gates at 80.5° N, 79.5° N and 79° N, respectively.

summer minimum SIE will turn into MYI at the onset of the growth season (see the 40th week in Fig. 1). While after movement during the growth season, the position of those MYI can change significantly (compare the SIA and the black lines in the 10th week in Fig. 1). Some of them were outside of the summer minimum SIE edge of that year (compare the SIA and the

https://doi.org/10.1017/jog.2024.33 Published online by Cambridge University Press

white lines in the 10th week in Fig. 1), such as in 2007 and 2010. If those MYI keep being outside during the melt season, we can approximate that they were lost due to melt. Therefore, MYI grid-cells outside the summer minimum SIE at the onset of melt season (20th–25th weeks in our paper) will be used to estimate the MYI melt, assuming the MYI inflow and outflow through the summer minimum SIE edge are close during the melt season. We consider this assumption suitable for estimating melt based on the following two points. First, we found that the MYI extent within the summer minimum SIE edge changes mildly after the 25th week compared to our estimated melt in most years. Second, the estimated melt remains relatively stable in the calculation. When using individual weeks from 15th to 30th as the onset of the melt season for calculation, we found that the range of calculated melt is moderate comparing the results using the average of the 20th–25th weeks. Importantly, regardless of the chosen weeks (15th–30th weeks), the difference in average melt before and after 2007, as focused on in Section 4.3, remains similar in magnitude.

In our estimation method, a key factor is the relative position between the location of MYI at the onset of the melt season and the summer minimum SIE edge. The shrinkage of the summer minimum SIE edge to a certain degree signifies an intensification of the summer melting process, which can be attributed to thinner ice and warmer temperatures. Simultaneously, the location of the MYI during the melt season is also a crucial factor in determining whether it will disappear due to summer melting. For example, for the same MYI, it is much more likely to melt in the southern Beaufort Sea than in the central Arctic, especially in recent decades. Consequently, the transport of MYI during the growth season can also influence the MYI summer melting by adjusting the location of MYI at the onset of the melt season. Overall, the MYI melt estimated above is actually the combined interaction of dynamic and thermal processes.

This perception is analogous to the melt estimation method in Kwok and Cunningham (2010) and the 'survival zone' concept in Mallett and others (2021). Kwok and Cunningham (2010) have employed a novel method to estimate the MYI melt area in the Beaufort Sea. They propagate MYI pixels from 1 April using daily ice motion fields and regarded pixels as melting if they are located outside the daily ice edge after propagation. Mallett and others (2021) define a 'survival zone' as the area where sea ice is present on 1 September in more than 50% of the years over the last decade. They suppose that the unusually high export of MYI during the winter of 2020/21 to areas outside this survival zone (primarily the Beaufort Sea) might lead to greater MYI loss.

It should be noted that the actual MYI melt will be greater than our estimates, as our method does not account for MYI melt within the summer minimum SIE edge, which is associated with reduced SIC. This limitation will be further discussed in Section 5.

3.3 The residual term

The residual term may be composed of the influences of several factors, including the omission of the sea-ice export through other gates, such as the Nares Strait (see B23 for the estimations of export through other gates), the bias of our calculation in Sections 3.1 and 3.2, the sea-ice deformation process, along with other artificial or physical biases that we have not considered. Regarding the sea-ice deformation, the convergence of MYI reduces its extent, while simultaneously opening sea water and producing FYI during the growth season. The role of deformation process is also highlighted by Regan and others (2023) and considered as a sink in their MYI area budget using a sea-ice model. For the NSIDC-SIA dataset used here, we consider the MYI deformation and its effect on FYI production to be common. Specifically, the production of FYI can occur across most regions within MYI coverage (Fig. S3 provides an example of 2015/16) and can even be pronounced in the north of the Canadian Arctic Archipelago (CAA), where the oldest ice is situated (refer to Section 4.3 and Fig. S6). This may, to some extent, underscore the widespread occurrence and impact of MYI deformation.

4. Results

4.1 The stepwise shift of 4+ year ice extent in the Arctic Basin

Figures 2a and S4 show the evolution of the annual average (average over one growth–melt cycle) SIE of different ages during 1985–2022. From the perspective of linear trend during the whole period, a striking feature is the drastic and significant decreasing trend in the extent of 4+ year ice, with a rate of -0.82×10^6 km^2 decade^{-1} ($p < 0.01$; Fig. 2a). The extent of 3 year ice shows a non-significant decreasing trend, whereas the extent of 2 year ice exhibits a significant ($p < 0.05$) but moderate increasing trend (Fig. S4). This results in a non-significant trend in the extent of 2–3 year ice (Fig. 2a). Therefore, the evident decline in the MYI coverage reported in previous studies (e.g. Comiso, 2012; B23) might be primarily driven by the decline in the 4+ year ice. As mentioned previously, due to the below-freezing temperature, the greatly reduced MYI extent can be occupied by newly formed FYI in winter. Therefore, there is a significant increasing trend in the FYI extent, with a rate of 0.49×10^6 km^2 decade^{-1} ($p < 0.01$; Fig. 2a), which can largely offset the decrease of MYI, and thus limit the total loss of sea ice.

However, it is noteworthy that the changes of FYI and 4+ year ice extent are not gradual; instead, they exhibit stepwise characteristics before and after around 1990 and 2008, respectively. After the stepwise changes, the equilibrium states of FYI and 4+ year ice extent (gray-dashed lines in Fig. 2a), which represent the mean state of the sea-ice system after adjusting to climate forcing (Armour and others, 2011), have transitioned significantly from the former to the latter. The former stepwise change has been reported in many previous studies, which emphasize the key role of a shift in the Arctic Oscillation (AO) to high-index conditions (e.g. Belchansky and others, 2004; B23). The rise in the AO flushed MYI out of the Beaufort Gyre and into Transpolar Drift Stream, leading to increased MYI export. The latter stepwise change, which is the main focus of our investigation, has also been raised in recent studies (e.g. Sumata and others, 2023) and can be clearly identified using the 7 year moving t-test (Fig. 2b; similar results are obtained using 9 year and 11 year windows). After this stepwise shift, the FYI extent increased from $\sim 3.0 \times 10^6$ to $\sim 3.9 \times 10^6$ km^2, with its fraction relative to the total ice changing from 42.5 to 61.4%. Meanwhile, the extent of 4+ year ice decreased from $\sim 2.1 \times 10^6$ to $\sim 0.6 \times 10^6$ km^2, with its fraction changing from 30.5 to 10.0%.

The shift towards younger Arctic sea ice after 2008 is also evident in the SIA spatial distribution, as shown in Figures 2c–e. For the 4+ year ice, a noticeable decrease is observed across almost the entire western Arctic (0–180° W). Its decrease in the north of Greenland and the CAA has been primarily offset by an increase in 2–3 year ice in that region, while its decrease in the Pacific Arctic (purple box in Figs 2c, e) has been primarily offset by an increase in FYI. Additionally, the 2–3 year ice exhibits a decrease in the Arctic Ocean more toward Eurasia, which has been offset by an increase in FYI there. The dipole feature of the change in 2–3 year ice eventually explains a non-significant trend of its extent (Fig. 2a). Overall, after this stepwise shift, sea ice in most regions of the Arctic has been occupied by younger ice, with the most pronounced changes in the Pacific Arctic (purple box in Figs 2c, e).

https://doi.org/10.1017/jog.2024.33 Published online by Cambridge University Press

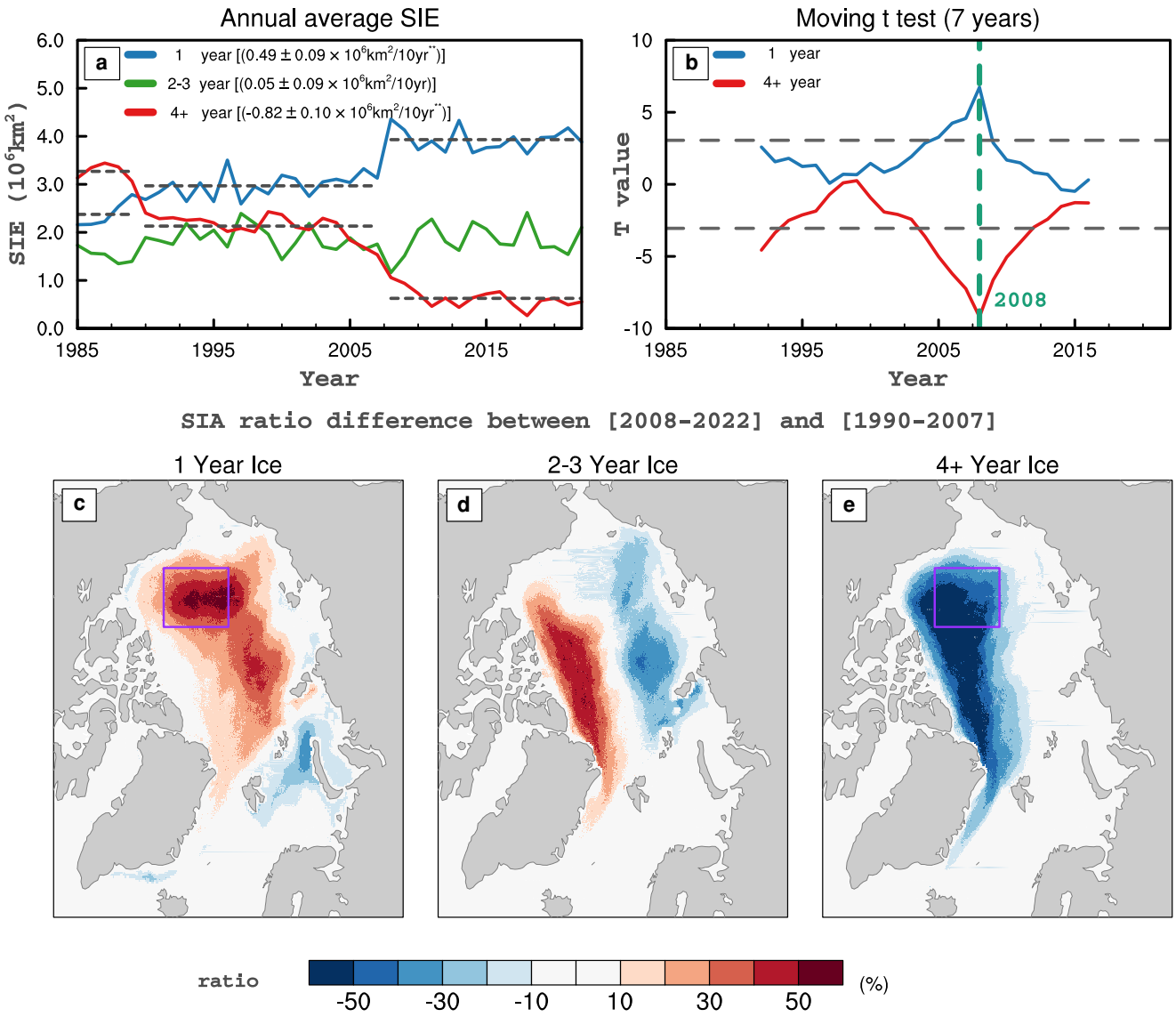

Figure 2. (a) Evolution of the annual average sea ice extent (SIE) of different ages during 1985–2022. The gray-dashed lines represent the equilibrium states of first year ice (FYI) and 4+ year ice during three periods (1985–89, 1990–2007 and 2008–22), respectively. The brackets indicate the slopes and their 95% significance limits. One and two asterisks represent the slopes exceeding 95 and 99% significance levels, respectively. (b) The 7 year moving *t*-test results of 4+ year ice extent and FYI extent. The gray-dashed line indicates the 99% significance level. (c–e) The difference in the ratio of each gridcell occupied by certain SIA between 2008–22 and 1990–2007. The purple box signifies where the 4+ year ice has been obviously replaced by the FYI.

4.2 The control from the decreased survivability

Considering the increase of FYI as an offset to the decline of MYI, which is primarily attributed to the loss of 4+ year ice, our focus here will be on exploring the stepwise decrease of 4+ year ice extent. In the previous subsection, we mentioned that there was no significant trend in the extent of 3 year ice during 1985–2022, whereas the extent of 4+ year ice showed a significant decline after 2008. Therefore, we can reasonably speculate that it is the decrease of survivability that drives less sea ice entering or remaining in the 4+ year ice. As described in Section 2.2, we can calculate the survival ratio of 3+ year ice extent $\beta_{3^+,\,n}$ and its counterpart in growth season $\beta^{\text{growth}}_{3^+,\,n}$ and melt season $\beta^{\text{melt}}_{3^+,\,n}$. We will have:

$$SIE_{4^+,\,(n,\,St^{\text{th}})} = \beta_{3^+,\,n} \times SIE_{3^+,\,(n-1,\,St^{\text{th}})} \quad (6)$$

Figures 3a and b show the evolution of three survival ratios during 1985–2022 and their 7 year moving *t*-test results. It is evident that the $\beta_{3^+,\,n}$ exhibits stepwise decrease since 2007, which is 1 year earlier than the shift year of the annual average SIE of 4+ year ice (see Fig. 2b; i.e. 2008). Indeed, this 1 year earlier relationship is expected. According to Eqn (6), it is the survival ratio in the n year ($\beta_{3^+,\,n}$) that determines the 4+ year ice extent at the onset of $n+1$ year ($SIE_{4^+,\,(n,\,St^{\text{th}})}$), which can highly capture the variability of the annual average 4+ year ice extent in the $n+1$ year (their correlation coefficients are 0.99 and 0.93 for non-detrend and detrended time series). During 1989–2006, the mean state of $\beta_{3^+,\,n}$ stood at ~71.7%. However, it significantly decreased to 47.0% after 2007 ($p < 0.01$, two-sample *t*-test). The stepwise decrease of $\beta_{3^+,\,n}$ was mainly driven by the decrease of its melt season counterpart $\beta^{\text{melt}}_{3^+,\,n}$, which also exhibited a stepwise decrease since 2007. The $\beta^{\text{growth}}_{3^+,\,n}$ also exhibits a significant stepwise decrease, albeit 3 years later (around 2010), thus contributing to the decrease of $\beta_{3^+,\,n}$ as well. Additionally, it is noteworthy that enhanced interannual variability has also been observed in all survivability metrics since 2007 (Fig. 3a). The decrease of $\beta^{\text{growth}}_{3^+,\,n}$ and $\beta^{\text{melt}}_{3^+,\,n}$ suggests the combined impact of dynamic and thermodynamic processes on the decrease of $\beta_{3^+,\,n}$. The contribution of specific processes will be estimated in the next subsection. Subsequently, we will quantify the relationship between the stepwise decrease of $SIE_{4^+,\,(n,\,St^{\text{th}})}$ and $\beta_{3^+,\,n}$.

https://doi.org/10.1017/jog.2024.33 Published online by Cambridge University Press

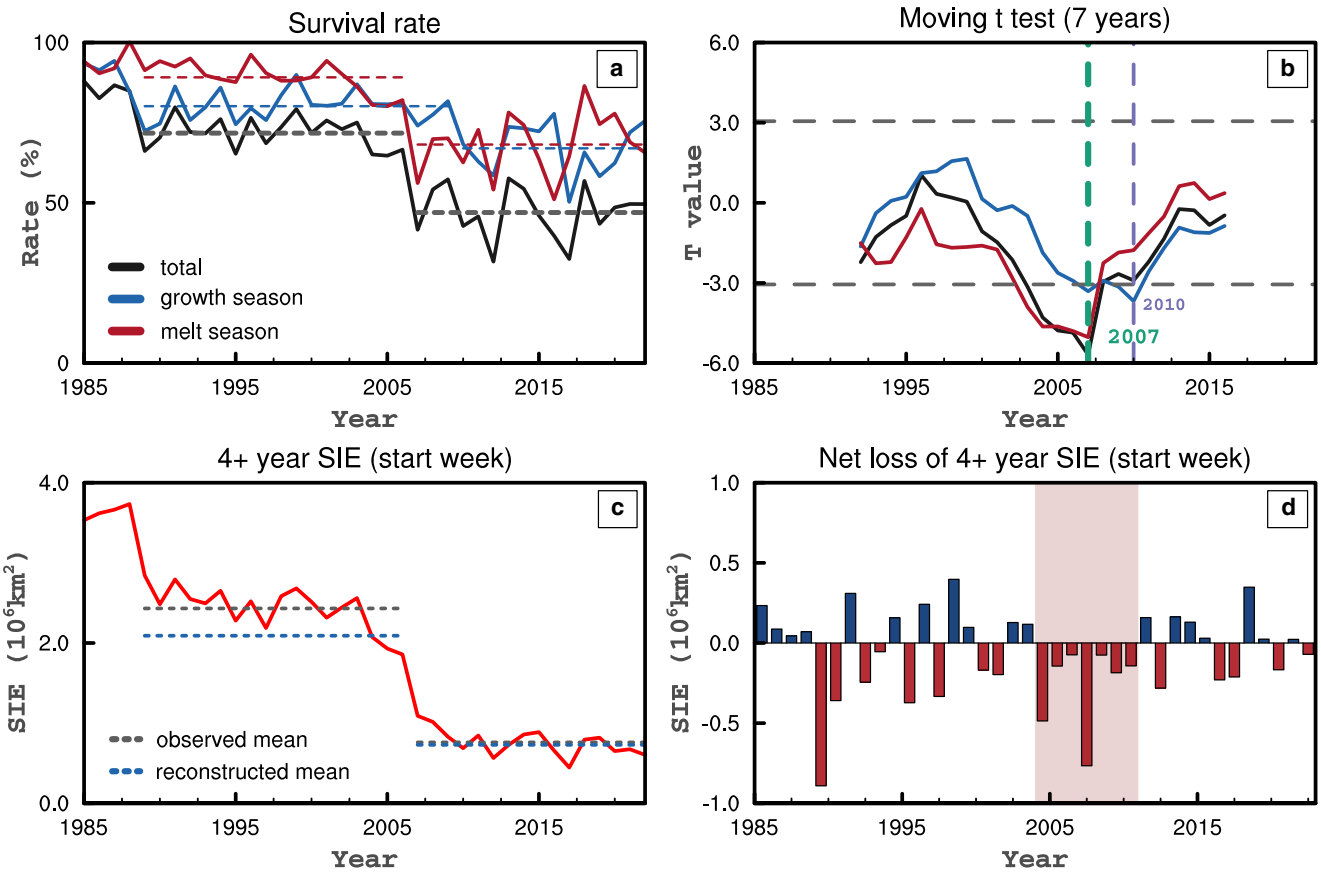

Figure 3. (a) Survival ratio of 3+ year ice in the growth season (blue line), the melt season (red line) and the whole growth–melt cycle (black line) during 1985–2022. The gray- and red-dashed lines represent the averages of the survival ratio over the periods 1989–2006 and 2007–22, while the blue-dashed line shows the averages for 1989–2009 and 2010–22. (b) The 7-year moving *t*-test of survival ratio in (a). The gray-dashed lines represent the 99% confidence level. (c) The extent of 4+ year ice in the start week during 1985–2022. The gray and blue lines indicate the observed and reconstructed mean of period 1989–2006 and 2007–22, respectively. (d) The net loss of 4+ year ice extent in the start week. Red shading region represents the period of 2004–10.

First, we have:

$$SIE_{3^+,\,(n-1,\,St^{th})} = SIE_{3,\,(n-1,\,St^{th})} + SIE_{4^+,\,(n-1,\,St^{th})}. \quad (7)$$

Following Armour and others (2011), we can decompose each variable into equilibrium and perturbation components: $A_n = \bar{A} + A'_n$. The equilibrium represents the mean state before and after the shift mentioned above. The perturbation represents deviations from the equilibrium state, equivalent to interannual variations. Substituting Eqn (7) into Eqn (6) and considering only the equilibrium state, we will have:

$$\overline{SIE_{4^+,\,St^{th}}} = \overline{SIE_{3,\,St^{th}}} \times \frac{\overline{\beta_{3^+}}}{1-\overline{\beta_{3^+}}}. \quad (8)$$

Equation (8) reveals a non-linear relationship between $\overline{SIE_{4^+,\,St^{th}}}$ and $\overline{\beta_{3^+}}$. This non-linear relationship signifies that the reduction rate in $\overline{SIE_{4^+,\,St^{th}}}$ could be several times greater than the reduction rate in $\overline{\beta_{3^+}}$. Specifically, for the equilibrium state of 1989–2006, where $\overline{\beta_{3^+}} = 71.7\%$, $\overline{SIE_{4^+,\,St^{th}}}$ will be 2.53 times the $\overline{SIE_{3,\,St^{th}}}$. In comparison, for the equilibrium state of 2007–22, where $\overline{\beta_{3^+}} = 47.0\%$, $\overline{SIE_{4^+,\,St^{th}}}$ will reduce to only 0.89 times the $\overline{SIE_{3,\,St^{th}}}$. With Eqn (8), we can reconstruct $\overline{SIE_{4^+,\,St^{th}}}$ over 1990–2007 and 2008–22 by substituting $\overline{SIE_{3,\,St^{th}}}$ and $\overline{\beta_{3^+}}$ into it. Given that the extent of 3 year ice exhibits no significant trend, its average value over 1985–2022 was used to substitute for $\overline{SIE_{3,\,St^{th}}}$. Then $\overline{\beta_{3^+}}$ in periods over 1989–2006 and 2007–22 were substituted into Eqn (8), respectively, to obtain $\overline{SIE_{4^+,\,St^{th}}}$ in their corresponding periods. The outcomes indicate that the reconstructed $\overline{SIE_{4^+,\,St^{th}}}$ can capture the shift observed between two periods (Fig. 3c), validating Eqn (8) and highlighting the role of decreased $\overline{\beta_{3^+}}$ in controlling the decline of $\overline{SIE_{4^+,\,St^{th}}}$.

Figure 3d shows the net loss/replenishment of 4+ year ice extent ($SIE_{4^+,\,(n,\,St^{th})} - SIE_{4^+,\,(n-1,\,St^{th})}$), which predominantly displays characteristics of interannual oscillations. These oscillations are possibly related to the negative feedback of SIE (Notz and Marotzke, 2012), where most strong negative year-to-year change in SIE is followed by a positive year-to-year change and vice versa. Notably, a sustained net loss is observed during the period 2004–10. Here, this period could be considered as a transition period from a regime with relatively high $\overline{\beta_{3^+}}$ (1989–2006) to a regime with relatively low $\overline{\beta_{3^+}}$ (2007–22). Specifically, lower $\overline{\beta_{3^+}}$ represents greater loss and less replenishment for the 4+ year ice extent. As a result, the 4+ year ice extent must reduce to a certain degree to achieve a balance between its loss and replenishment, thereby maintaining an equilibrium state as demonstrated by Eqn (8). Therefore, rather than regarding the sustained loss during 2004–10 as a cause, it is the relatively low $\overline{\beta_{3^+}}$ since 2007 that has controlled or maintained the relatively low 4+ year ice extent.

4.3 The contribution of various processes on the decrease of survivability

Then how have various processes contributed to the decrease of $\overline{\beta_{3^+}}$ since 2007? As described in Section 3, we will first illustrate the MYI loss of each SIA due to export through FS and summer melting (Fig. 4), and then focus on their loss rate concerning the budget of $\overline{\beta_{3^+}}$ (loss divided by $SIE_{3^+,\,(n-1,\,St^{th})}$; Fig. 5).

https://doi.org/10.1017/jog.2024.33 Published online by Cambridge University Press

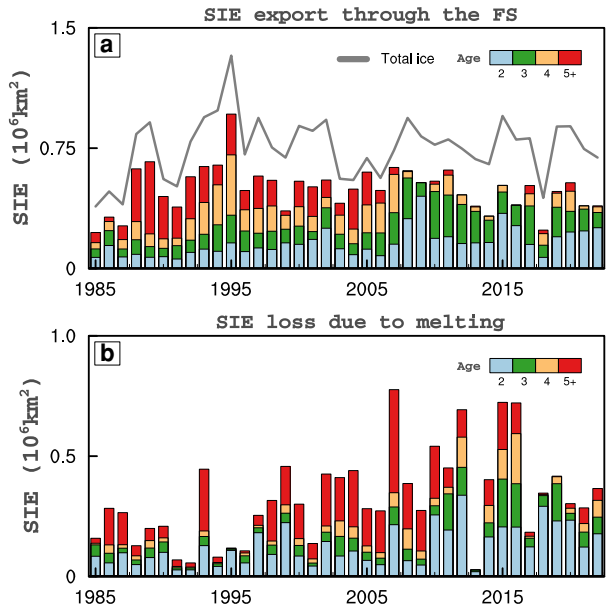

Figure 4. Multi-year ice extent loss due to (a) export through Fram Strait and (b) summer melting during 1985–2022. The gray line in (a) indicates the export flux of total ice (FYI and MYI).

The average annual area export of total ice (including MYI and FYI) through the FS is $\sim 0.75 \times 10^6\,\mathrm{km}^2$ (Fig. 4a), with MYI accounting for 66% ($0.50 \times 10^6\,\mathrm{km}^2$). This proportion closely aligns with the findings (67%) reported by Wang and others (2022), although they identify the MYI based on satellite products during 2002–20. Additionally, the results are not sensitive to the location of the gate (Fig. S5). Notably, since around 2007, the 2–3 year ice flux has dominated the MYI flux, while the flux of 4+ year ice accounts for only a minor proportion. Furthermore, over our study period, the MYI proportion in export through FS decreased significantly at a rate of −4% ($p = 0.015$; not shown). Therefore, the ice export through FS has become younger, which could be due to the contraction of MYI away from FS towards the north of CAA (Krumpen and others, 2019; B23).

For the MYI loss due to summer melting, its annual average is $\sim 0.32 \times 10^6\,\mathrm{km}^2$ (Fig. 4b). Before around 2010, the MYI melt was mainly 5+ year ice, but after that, it shifted to being primarily composed of 2–3 year ice. In 2013, our estimated MYI melt was extremely low. This is because the summer minimum extent edge in 2013 was more extensive than the previous few years, and simultaneously, few MYI were moving outside of it during the growth season (Fig. 1; Perovich and others, 2013). This low melt is consistent with a relatively high sea-ice volume in 2013 (Tilling and others, 2015). Again, it is important to note that the estimated MYI melt presented here and below does not account for MYI melt within the summer minimum edge (see Sections 3.2 and 5), and therefore, may underestimate the actual MYI melt area.

Regarding the loss rate driven by the export of 3+ year ice through the FS, no significant trend has been observed since the early 1990s (Fig. 5a). Moreover, there is only a modest increase before and after 2007 (12.6 vs 15.4%; Fig. 5e), suggesting that the export through FS may not be a primary contributor to the decrease of $\overline{\beta_{3+}}$ since 2007.

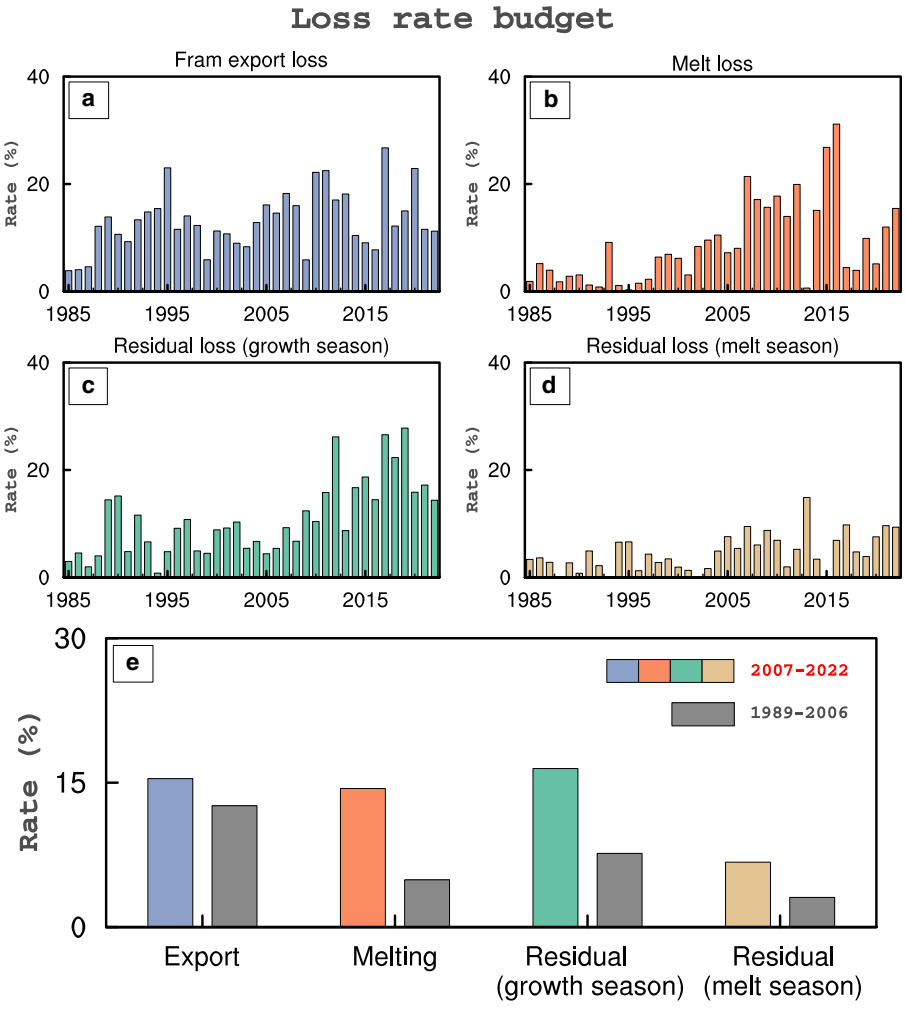

Figure 5. The 3+ year ice loss rate during 1985–2022 contributed by (a) export through FS, (b) summer melting, (c) residual part in the growth season and (d) residual part in the melt season. (e) Comparison in the average loss rate between 1989–2006 and 2007–22.

https://doi.org/10.1017/jog.2024.33 Published online by Cambridge University Press

For the melt rate of 3+ year ice, there was an evident increase during 2007–16, although it appeared to rebound back in recent years (Fig. 5b). The average melt rate has significantly risen from 4.9 to 14.3% before and after 2007 (Fig. 5e). Consequently, we can attribute the intensified summer melting as a main contributor to the decrease of $\overline{\beta_{3+}}$. As stated in Section 3.2, it is worth emphasizing that the estimated melt primarily consists of those 3+ year ice that move to regions that are relatively warm and hard to survive, such as the Beaufort Sea and Chukchi Sea, rather than where they formed. Specifically, during 1989–2006, the summer minimum extent edge is relatively more extensive, and there is only limited 3+ year ice located outside of the edge at the onset of melt season (Fig. 6a). Consequently, the amount of melted 3+ year ice is expected to be relatively small. In contrast, after 2007, the summer minimum extent edge has significantly shrunk, especially in the Pacific Arctic (compare the white lines in Figs 6a, b), corresponding to intensified melting. However, as a permanent system, the Beaufort Gyre could consistently transport 3+ year ice from the north of CAA to the Beaufort and Chukchi seas during the growth season. This process can be clearly indicated by the westward extension of the tongue of MYI drawn through the Beaufort Gyre (see shading in Fig. 6b and the 10th week in Fig. 1). Since the MYI typically cannot survive through the Beaufort Gyre in recent periods (Maslanik and others, 2007; Kwok, 2018; Babb and others, 2022), the loss rate of melt is expected to increase. In addition, the Beaufort Gyre has strengthened during the growth season since 2007, as indicated by the vectors in Figure 6c. This strengthening may be associated with dipole sea-level pressure anomaly patterns (contours in Fig. 6c) and decreasing ice thickness (Rampal and others, 2009). Consequently, this enhanced Gyre can transport more 3+ year ice to the Beaufort and Chukchi seas, where the summer 2 m air temperature has warmed noticeably since 2007 (shading in Fig. 6c), possibly helping more melt.

The residual loss rate during the growth season shows a noticeable increase after 2011 (Fig. 5c), corresponding to the stepwise decrease of $\beta_{3+,\,n}^{\text{growth}}$ since 2010. Before and after 2007, it has increased from 7.7 to 16.5% (Fig. 5e), thus also largely contributing to the decrease of $\overline{\beta_{3+}}$. The residual loss rate during the melt season is relatively small compared to its counterpart in the growth season, exhibiting an increase from 3.1 to 6.7% before and after 2007 (Figs 5d, e). While the exact causes of the increased residual term remain uncertain, we speculate that increasing

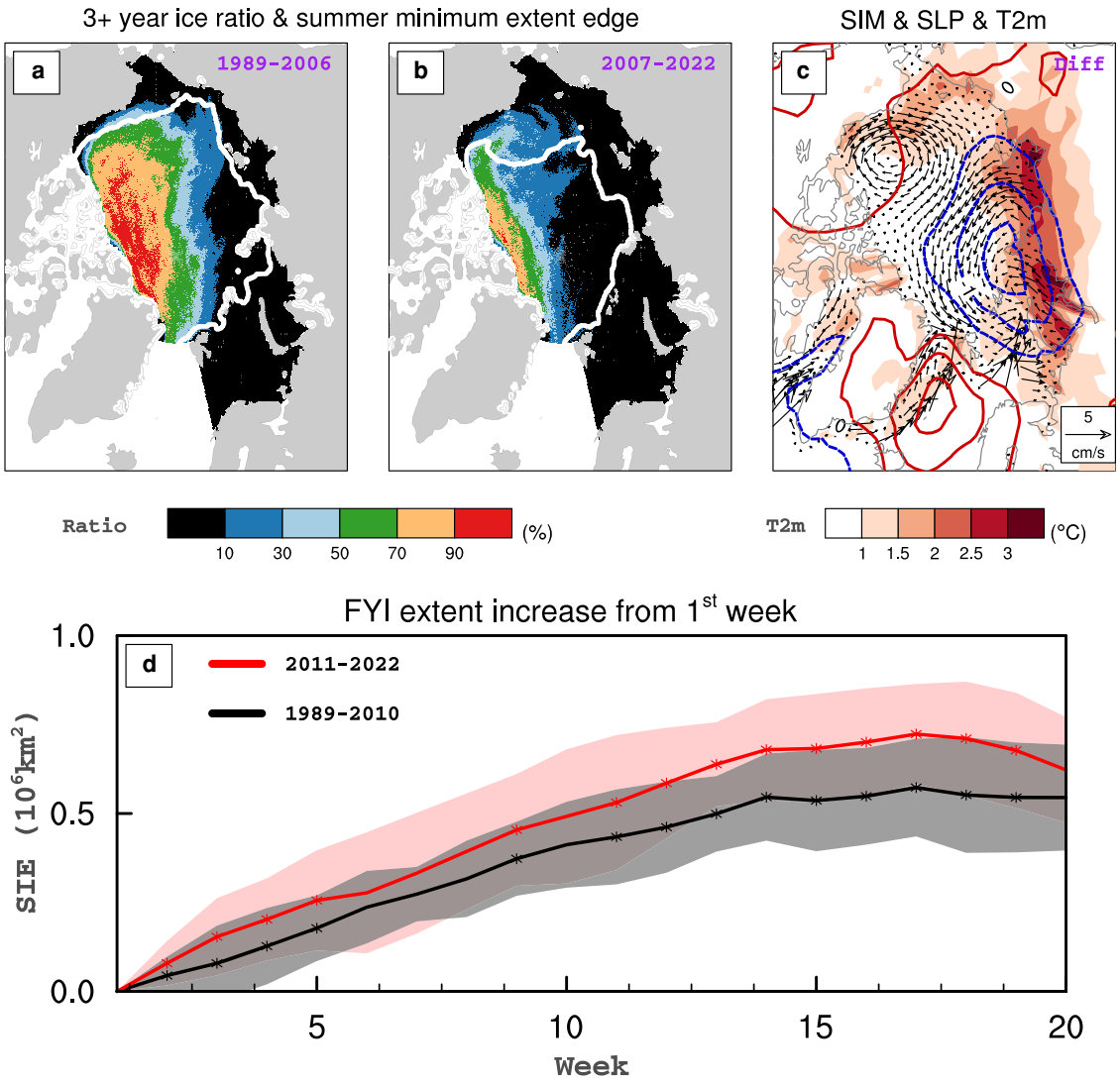

Figure 6. Ratio of each gridcell occupied by 3+ year ice at the onset of melt season (20th–25th weeks) during (a) 1989–2006 and (b) 2007–22. The white line indicates the averaged summer minimum SIE during corresponding periods. (c) The difference of SIM (vectors) and sea-level pressure averaged over January–May (contours), and 2 m air temperature averaged over August–September (shading) between 2007–22 and 1989–2006. (d) The increase of FYI extent from 1st week (1–7 January) averaged over 2011–22 (red line) and 1989–2010 (black line). The asterisks indicate where their difference is significant ($p < 0.1$; two-sample *t*-test). The shadings represent the range of one std dev.

https://doi.org/10.1017/jog.2024.33 Published online by Cambridge University Press

sea-ice deformation processes, which are related to ice becoming thinner and more dynamic (Rampal and others, 2009; Zhang and others, 2012), may have played a role. For the MYI, its export through FS and convergence can both reduce its area but produce FYI during winter (see also Section 3.3). Since 2011, the FYI production during winter in the Arctic Basin has significantly increased compared to before (Fig. 6d). Notably, this increase can even be evident in the north of CAA (Fig. S6), where is dominated by the oldest ice in the Arctic. Given that the MYI export through FS exhibits a decreasing trend since 2011 (Fig. 4a), we consider that the increased FYI production during winter since 2011 may serve as potential evidence of the strengthened deformation process of MYI, thereby contributing to the increased residual term during the growth season. Detailed examinations of these processes are a promising avenue for future research.

5. Discussion

In the analysis above, we utilized the SIE, which essentially represents the number of corresponding pixels, to quantify the change of 4+ year ice. However, it is important to note that since the SIA was assigned to the oldest parcel within its pixel, the extent of 4+ year ice inherently overestimates its true area. To a certain degree, this bias does hinder our quantitative exploration, such as determining the specific proportion by which the 4+ year ice reduced after 2007. However, for the primary purpose of our study, which is to reflect potential regime shifts around 2007 in the Arctic climate system, we consider this overestimation bias to be acceptable.

First, the shift year (around 2007) derived from 4+ year ice extent aligns well with other studies, such as B23. They also use the NSIDC-SIA dataset, while additionally considering the SIC and using it to calculate the summer minimum MYI area. Second, the loss of 4+ year ice pixels (extent), while not directly indicative of the true reduction in area, does signify that all 4+ years ice parcels within the pixel have been lost by some processes. Therefore, the loss of extent can offer insight into the persistence of pixels containing 4+ years ice. This is also why we employed the sea-ice survivability concept from Armour and others (2011) into our analysis, which can reflect the forcing of other factors on the persistence of sea ice, thereby providing insights into changes in Arctic thermodynamic and dynamic regimes.

Furthermore, we computed the ratio of 3+ year ice pixels with SIC >50% in the start week (Fig. 7). We find it can be maintained at relatively high levels (with a minimum of ~84%) despite showing some decline and increased variability since 2000. This indicates that the 3+ years ice pixels we focus on will not be dominated by the physical properties of newly formed FYI during winter. More importantly, the average ratios between the two periods focused on in our paper (1989–2006 and 2007–22) are not substantially different (95 vs 92%). Comparable differences can be achieved by computing the ratio of SIC >60% (92 vs 88%) or 70% (84 vs 81%).

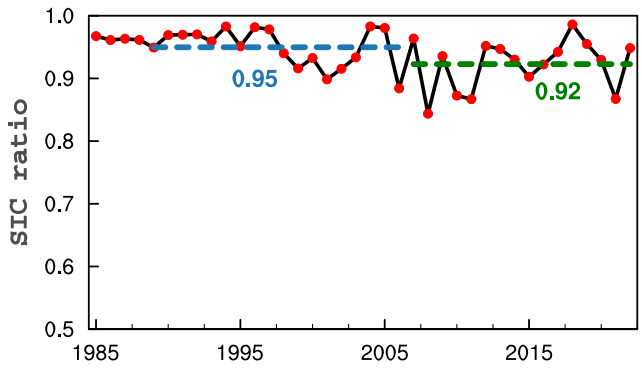

Figure 7. Ratio of 3+ year ice pixels with their sea-ice concentration (SIC) >50% relative to the total 3+ year ice pixels in the start week. Blue- and green-dashed lines indicate the averages for 1989–2006 and 2007–22, respectively.

We also compared our estimated MYI melt extent with the MYI melt area calculated by B23 (Fig. S7). The correlation coefficient between them is 0.63. We attribute this high correlation to two points: first, they both exhibit an increasing trend, and second, their correspondence improves significantly after around 2007. As mentioned in Section 3.2, our melt term does not encompass losses associated with reduced SIC within the summer minimum extent. We consider this might be a possible reason for the discrepancy between our melt term and B23 before 2007. During this period, the summer minimum extent is relatively extensive (Fig. 6a), and thus the effect of reduced SIC might predominate for the melt term. However, during post-2007, the summer minimum extent has shrunk significantly (Fig. 6b), making MYI melt due to propagation to marginal seas, where it is challenging for sea ice to survive the summer transit, more dominant. Based on this comparison, we believe that our estimated older MYI extent loss due to summer melting can reasonably reflect significant changes in the melting process between the periods before and after 2007, although there might be differences compared to the actual melt area.

Overall, given the presence of the overestimation bias, we consider the results obtained in our paper to be semiquantitative but reasonable. These findings can be helpful for us to understand potential changes in the Arctic climate system within the regime shift around 2007, especially considering the current lack of datasets which can detail the SIC of each age within a pixel. For instance, we propose that the role of summer melting may be more pivotal than that of FS export in the stepwise decrease of 4+ year ice, although their specific contributions may still entail some uncertainty. Additionally, if long-term datasets similar to Korosov and others (2018), containing corresponding SIC for different ages of sea ice, becomes available in the future, it can be used to validate and complement our study.

6. Summary

Using the NSIDC-SIA dataset, this study revealed that the rapid decline in MYI coverage reported by previous studies (e.g. Kwok, 2018) might be primarily attributed to the decrease in 4+ year ice. Moreover, it is important to emphasize that the 4+ year ice extent decreased stepwise before and after 2008 (2007 summer), instead of decreasing gradually. After this shift, the 4+ year ice extent changed from 2.1×10^6 to 0.6×10^6 km^2, with its fraction relative to the total ice changing from 30.5 to 10.0%. The shift of SIA towards younger is evident in most regions of the Arctic, with the most pronounced in the Pacific Arctic (purple box in Fig. 2c).

The decrease of 4+ year ice extent reflects the fact that less ice entering or remaining in the 4+ year ice group. Therefore, the stepwise decrease of 4+ year ice is essentially a reflection of the reduced survivability of 3+ year ice (the survival part of 3+ year ice will become 4+ year ice in next year), which also decreases stepwise from 72.0 to 46.8% since around 2007. Analyzing the decrease in the 4+ year ice extent from the perspective of survivability provides us with two important insights: (1) when considering the equilibrium state, the 4+ year ice extent is controlled by the survivability of 3+ year ice in a non-linear manner, as indicated by Eqn (8). This highlights that small alterations in the survivability can result in relatively large changes in the extent; (2) rather than regarding the sustained loss during 2004–10 (Fig. 3d) as a cause, it is the relatively low survivability since 2007 that has maintained

https://doi.org/10.1017/jog.2024.33 Published online by Cambridge University Press

the relatively low 4+ year ice extent, and also has maintained it to not drop to a new lower level.

The decrease in the survivability of 3+ year ice is driven by both the winter and summer processes. The most substantial contribution to the decreased survivability comes from the intensified summer melting (38.1%). The increase in the export through FS is relatively minor and thus not a major factor. However, the significant rise in residual loss during the growth season suggests that other winter processes, such as sea-ice deformation, may have played a significant role in it.

The stepwise decrease in the 4+ year ice extent and its linked survivability could serve as evidence of a regime shift around 2007 within the arctic climate system, as revealed by recent studies (e.g. Polyakov and others, 2023; Sumata and others, 2023). The stepwise variation feature could help to interpret the recent slowdown in the decline of summer Arctic sea ice (Francis and Wu, 2020; Zhang, 2021). It is worth noting that the 4+ year ice extent comprises only ~20% of total MYI since 2008, suggesting that an evident decrease in the September sea-ice coverage (equivalent to MYI coverage) will need a decrease in the 2–3 year ice.

Supplementary material. The supplementary material for this article can be found at https://doi.org/10.1017/jog.2024.33

Acknowledgements. This study was supported by the National Key Research and Development Program of China (grant No. 2022YFE0106800), the Natural Science Foundation of China (NSFC) (grant No. 42230603) and the Innovation Group Project of the Southern Marine Science and Engineering Guangdong Laboratory (Zhuhai) (grant No. 311021001). We thank David Babb and one anonymous reviewer for their careful reading of our manuscript and their insightful suggestions.

References

Armour KC, Bitz CM, Thompson L and Hunke EC (2011) Controls on Arctic sea ice from first-year and multiyear ice survivability. *Journal of Climate* **24**(9), 2378–2390. doi: 10.1175/2010JCLI3823.1

Babb DG and 5 others (2022) Increasing multiyear sea ice loss in the Beaufort Sea: a new export pathway for the diminishing multiyear ice cover of the Arctic ocean. *Geophysical Research Letters* **49**(9), e2021GL097595. doi: 10.1029/2021GL097595

Babb DG and 8 others (2023) The stepwise reduction of multiyear sea ice area in the Arctic ocean since 1980. *Journal of Geophysical Research: Oceans* **128** (10), e2023JC020157. doi: 10.1029/2023JC020157

Belchansky GI, Douglas DC and Platonov NG (2004) Duration of the Arctic sea ice melt season: regional and interannual variability, 1979–2001. *Journal of Climate* **17**(1), 67–80. doi: 10.1175/1520-0442(2004)017<0067:DOTASI>2.0.CO;2

Bi H and 9 others (2020) Arctic multiyear sea ice variability observed from satellites: a review. *Journal of Oceanology and Limnology* **38**(4), 962–984. doi: 10.1007/s00343-020-0093-7

Comiso JC (2012) Large decadal decline of the Arctic multiyear ice cover. *Journal of Climate* **25**(4), 1176–1193. doi: 10.1175/JCLI-D-11-00113.1

DiGirolamo NE, Parkinson CL, Cavalieri DJ, Gloersen P and Zwally HJ (2022) Sea Ice Concentrations from Nimbus-7 SMMR and DMSP SSM/I-SSMIS Passive Microwave Data, Version 2. Boulder, CO, USA. NASA National Snow and Ice Data Center Distributed Active Archive Center. doi: 10.5067/MPYG15WAA4WX

Francis JA and Wu B (2020) Why has no new record-minimum Arctic sea-ice extent occurred since September 2012? *Environmental Research Letters* **15** (11), 114034. doi: 10.1088/1748-9326/abc047

Hersbach H and 42 others (2020) The ERA5 global reanalysis. *Quarterly Journal of the Royal Meteorological Society* **146**(730), 1999–2049. doi: 10.1002/qj.3803

Korosov AA and others (2018) A new tracking algorithm for sea ice age distribution estimation. *The Cryosphere* **12**(6), 2073–2085. doi: 10.5194/tc-12-2073-2018

Krumpen T and others (2019) Arctic warming interrupts the transpolar drift and affects long-range transport of sea ice and ice-rafted matter. *Scientific Reports* **9**(1), 5459. doi: 10.1038/s41598-019-41456-y

Kwok R (2007) Near zero replenishment of the Arctic multiyear sea ice cover at the end of 2005 summer. *Geophysical Research Letters* **34**(5), L05501. doi: 10.1029/2006GL028737

Kwok R (2015) Sea ice convergence along the Arctic coasts of Greenland and the Canadian Arctic archipelago: variability and extremes (1992–2014). *Geophysical Research Letters* **42**(18), 7598–7605. doi: 10.1002/2015GL065462

Kwok R (2018) Arctic sea ice thickness, volume, and multiyear ice coverage: losses and coupled variability (1958–2018). *Environmental Research Letters* **13**(10), 105005. doi: 10.1088/1748-9326/aae3ec

Kwok R and Cunningham GF (2010) Contribution of melt in the Beaufort Sea to the decline in Arctic multiyear sea ice coverage: 1993–2009. *Geophysical Research Letters* **37**(20), L20501. doi: 10.1029/2010GL044678

Liu J and 13 others (2019) Towards reliable Arctic sea ice prediction using multivariate data assimilation. *Science Bulletin* **64**(1), 63–72. doi: 10.1016/j.scib.2018.11.018

Mallett RDC and 9 others (2021) Record winter winds in 2020/21 drove exceptional Arctic sea ice transport. *Communications Earth & Environment* **2**(1), 1–6. doi: 10.1038/s43247-021-00221-8

Maslanik J and 6 others (2007) A younger, thinner Arctic ice cover: increased potential for rapid, extensive sea-ice loss. *Geophysical Research Letters* **34** (24), L24051. doi: 10.1029/2007GL032043

Maslanik J, Stroeve J, Fowler C and Emery W (2011) Distribution and trends in Arctic sea ice age through spring 2011. *Geophysical Research Letters* **38** (13), L13502. doi: 10.1029/2011GL047735

Moore GWK, Steele M, Schweiger AJ, Zhang J and Laidre KL (2022) Thick and old sea ice in the Beaufort Sea during summer 2020/21 was associated with enhanced transport. *Communications Earth & Environment* **3**(1), 1–11. doi: 10.1038/s43247-022-00530-6

Notz D and Marotzke J (2012) Observations reveal external driver for Arctic sea-ice retreat. *Geophysical Research Letters* **39**(8), L08502. doi: 10.1029/2012GL051094

Perovich D and 6 others (2013) Sea Ice [in Arctic Report Card 2013]. *Arctic Report Card* 2013.

Polyakov IV and 7 others (2023) Fluctuating Atlantic inflows modulate Arctic atlantification. *Science* **381**(6661), 972–979. doi: 10.1126/science.adh5158

Rampal P, Weiss J and Marsan D (2009) Positive trend in the mean speed and deformation rate of Arctic sea ice, 1979–2007. *Journal of Geophysical Research: Oceans* **114**(C5), C05013. doi: 10.1029/2008JC005066

Regan H, Rampal P, Ólason E, Boutin G and Korosov A (2023) Modelling the evolution of Arctic multiyear sea ice over 2000–2018. *The Cryosphere* **17** (5), 1873–1893. doi: 10.5194/tc-17-1873-2023

Sumata H, De Steur L, Divine DV, Granskog MA and Gerland S (2023) Regime shift in Arctic ocean sea ice thickness. *Nature* **615**(7952), 443–449. doi: 10.1038/s41586-022-05686-x

Thomas DN (2017) *Sea ice*, 3rd edn. Chichester, UK: John Wiley & Sons, Hoboken, NJ.

Tilling RL, Ridout A, Shepherd A and Wingham DJ (2015) Increased Arctic sea ice volume after anomalously low melting in 2013. *Nature Geoscience* **8** (8), 643–646. doi: 10.1038/ngeo2489

Tooth M and Tschudi M (2018) Investigating Arctic sea ice survivability in the Beaufort Sea. *Remote Sensing* **10**(2), 267. doi: 10.3390/rs10020267

Tschudi MA, Stroeve JC and Stewart JS (2016) Relating the age of Arctic sea ice to its thickness, as measured during NASA's ICESat and IceBridge campaigns. *Remote Sensing* **8**(6), 457. doi: 10.3390/rs8060457

Tschudi MA, Meier W, Stewart J, Fowler C and Maslanik J (2019a) EASE-Grid Sea Ice Age, Version 4. Boulder, CO, USA. NASA National Snow and Ice Data Center Distributed Active Archive Center. doi: 10.5067/UTAV7490FEPB

Tschudi MA, Meier W, Stewart J, Fowler C and Maslanik J (2019b) Polar pathfinder daily 25 km EASE-grid sea ice motion vectors, version 4. Boulder, CO, USA. NASA National Snow and Ice Data Center Distributed Active Archive Center. doi: 10.5067/INAWUWO7QH7B

Tschudi MA, Meier WN and Stewart JS (2020) An enhancement to sea ice motion and age products at the National Snow and Ice Data Center (NSIDC). *The Cryosphere* **14**(5), 1519–1536. doi: 10.5194/tc-14-1519-2020

Wang Y, Bi H and Liang Y (2022) A satellite-observed substantial decrease in multiyear ice area export through the Fram Strait over the last decade. *Remote Sensing* **14**(11), 2562. doi: 10.3390/rs14112562

Yang Y and 5 others (2023) The evolution of the Fram Strait sea ice volume export decomposed by age: estimating with parameter-optimized sea

ice-ocean model outputs. *Environmental Research Letters* **18**(1), 014029. doi: 10.1088/1748-9326/acaf3b

Ye Y and 8 others (2023) Inter-comparison and evaluation of Arctic sea ice type products. *The Cryosphere* **17**(1), 279–308. doi: 10.5194/tc-17-279-2023

Zhang J (2021) Recent slowdown in the decline of Arctic sea ice volume under increasingly warm atmospheric and oceanic conditions. *Geophysical Research Letters* **48**(18), e2021GL094780. doi: 10.1029/2021GL094780

Zhang J, Lindsay R, Schweiger A and Rigor I (2012) Recent changes in the dynamic properties of declining Arctic sea ice: a model study. *Geophysical Research Letters* **39**(20), L20503. doi: 10.1029/2012GL053545

Zhao J, He S, Fan K, Wang H and Li F (2023) Projecting wintertime newly formed Arctic sea ice through weighting CMIP6 model performance and independence. *Advances in Atmospheric Sciences* **40**, 1–18. doi: 10.1007/s00376-023-2393-2

https://doi.org/10.1017/jog.2024.33 Published online by Cambridge University Press